

Rothamsted Repository Download

A - Papers appearing in refereed journals

Phillips, A. L., Huttly, A. K., Alarcon-Reverte, R., Clark, S. J., Jaworek, P., Tarkowska, D., Sokolowska, P., Steele, D., Riche, A. B., Hawkesford, M. J., Thomas, S., Hedden, P. and Pearce, S. 2025. GIBBERELLIN 3-OXIDASE genes regulate height and grain size in bread wheat. *Journal of Experimental Botany*. p. efa151. <https://doi.org/10.1093/jxb/eraf151>

The publisher's version can be accessed at:

- <https://doi.org/10.1093/jxb/eraf151>

The output can be accessed at:

<https://repository.rothamsted.ac.uk/item/99368/gibberellin-3-oxidase-genes-regulate-height-and-grain-size-in-bread-wheat>.

© 10 April 2025, Please contact library@rothamsted.ac.uk for copyright queries.

***GIBBERELLIN 3-OXIDASE* genes regulate height and grain size in bread wheat**

Andrew L. Phillips¹, Alison K. Huttly¹, Rocío Alarcón-Reverte¹, Suzanne J. Clark¹, Pavel Jaworek², Danuše Tarkowská², Patrycja Sokolowska¹, David Steele¹, Andrew Riche¹, Malcolm J. Hawkesford¹, Stephen G. Thomas¹, Peter Hedden^{1,2}, and Stephen Pearce^{1*}.

1. Rothamsted Research, Harpenden, Hertfordshire, AL5 2JQ, UK.
2. Laboratory of Growth Regulators, Institute of Experimental Botany, Czech Academy of Sciences and Palacký University Olomouc, Šlechtitelů 27, CZ-77900 Olomouc, Czech Republic.

* Corresponding author.

Email addresses:

Andrew L. Phillips: cycad@btinternet.com

Alison K. Huttly: arenga@btinternet.com

Rocío Alarcón-Reverte: rocio.alarcon-reverte@rothamsted.ac.uk

Suzanne J. Clark: suzanne.clark@rothamsted.ac.uk

Pavel Jaworek: jaworek.pavel@gmail.com

Danuše Tarkowská: tarkowska@ueb.cas.cz

Patrycja Sokolowska: patrycjasokolowska999@gmail.com

David Steele: david.steele@rothamsted.ac.uk

Andrew Riche: andrew.riche@rothamsted.ac.uk

© The Author(s) 2025. Published by Oxford University Press on behalf of the Society for Experimental Biology.

This is an Open Access article distributed under the terms of the Creative Commons Attribution License (<https://creativecommons.org/licenses/by/4.0/>), which permits unrestricted reuse, distribution, and reproduction in any medium, provided the original work is properly cited.

Malcolm J. Hawkesford: malcolm.hawkesford@rothamsted.ac.uk

Stephen G. Thomas: stephen.thomas.visiting@rothamsted.ac.uk

Peter Hedden: peter.hedden@rothamsted.ac.uk

Stephen Pearce: stephen.pearce@rothamsted.ac.uk

HIGHLIGHT

Characterization of the wheat GA 3-oxidase family revealed diversified functions. *GA3OX2* plays an essential and conserved role in vegetative and reproductive development, whereas variation in *GA3OX3/GA1OX1* genes affects grain development.

Accepted Manuscript

ABSTRACT

In plants, gibberellin (GA) levels are tightly regulated to optimise growth and development. GA 3-oxidases (GA3OX) catalyse a key GA biosynthesis step, converting precursor GAs into bioactive forms. We characterised seven *GA3OX* homologues in bread wheat (*Triticum aestivum* L.): a homoeologous triad of *GA3OX2* genes expressed in vegetative and reproductive tissues and four others (a homoeologous triad of *GA3OX3* genes plus *GA1OX1-B1*) expressed predominantly in grains.

ga3ox2 mutants are severely dwarfed and infertile due to very low bioactive GA levels, indicating *GA3OX2* is essential for normal wheat development. By contrast, *ga3ox3* mutants have lower bioactive GA levels in grains, reducing grain size and weight, while *galox1* mutants accumulate high levels of bioactive GAs, producing larger grains. Unexpectedly, *ga3ox3* and *galox1* alleles also affected height, possibly reflecting GA transport to vegetative tissues. Natural variation in adjacent *GA3OX3-B1* and *GA1OX1-B1* genes was associated with differences in grain size and weight, suggesting that a haplotype associated with larger grains was selected during modern breeding. Our study shows that the wheat *GA3OX* family has diversified roles, with *GA3OX2* required for general growth and *GA3OX3/GA1OX1* modulating GA levels during grain development. These findings highlight opportunities to exploit variation in GA biosynthetic pathways for wheat improvement.

KEYWORDS

Wheat, gibberellin, GA 3-oxidase, grain size, height, genetic diversity.

ABBREVIATIONS

2-ODD - 2-oxoglutarate-dependent dioxygenase

GA – gibberellin

GA20OX - GA 20-oxidase

GA2OX – GA 2-oxidase

GA3OX – GA 3-oxidase

EMS – ethyl methanesulfonate

LMM - linear mixed model

REML - Restricted maximum likelihood

TGW - thousand-grain weight

Accepted Manuscript

INTRODUCTION

Gibberellins (GAs) are a family of diterpenoid carboxylic acids, members of which function as hormone signals in higher plants, regulating important developmental processes such as seed germination, stem elongation, and flowering (Castro-Camba *et al.*, 2022). Of the 136 identified GA forms, only a few – primarily GA₁, GA₄ and GA₃ – exhibit bioactivity (Sponsel, 2016). These bioactive GAs bind the receptor GIBBERELLIN INSENSITIVE DWARF1 (GID1), triggering a conformational change that enhances the affinity of GID1 for DELLA proteins, resulting in the latter protein's polyubiquitination and degradation via the E3-ubiquitin ligase pathway (de Lucas *et al.*, 2008; Shimada *et al.*, 2008; Ueguchi-Tanaka *et al.*, 2005). DELLA proteins modulate the activity of hundreds of transcription factors through protein-protein interactions, and their GA-mediated degradation has a major effect on the cellular transcriptional landscape (Zentella *et al.*, 2007). Therefore, it is essential that bioactive GA levels are tightly controlled to ensure optimal growth responses to developmental signals and environmental cues (Shani *et al.*, 2024).

Plants precisely regulate bioactive GA levels through the activity of different classes of GA biosynthetic enzymes (Shani *et al.*, 2024). Four classes of 2-oxoglutarate-dependent dioxygenases (2-ODDs) – GA 20-oxidase, GA 3-oxidase, C₁₉-GA 2-oxidase and C₂₀-GA 2-oxidase – catalyse key steps in the final stages of GA biosynthesis (GA20OX and GA3OX) and inactivation (GA2OX) (Fig. 1). Each enzyme contains a conserved core domain that binds ferrous Fe (2+) as a cofactor that is required to catalyse the oxidation of GA substrates in the presence of the co-substrates O₂ and 2-oxoglutarate (Kawai *et al.*, 2014). Their activity is a major factor in determining the concentration of bioactive GAs.

The GA-biosynthetic pathway splits into the non-13-hydroxylation (13-H) or 13-hydroxylation (13-OH) branches depending on the 13-hydroxylation of GA₁₂ that is catalysed by the cytochrome P450 GA 13-oxidase (Fig. 1). In each branch, GA 20-oxidase (GA20OX) enzymes catalyse three consecutive oxidation reactions on C-20, producing GA₉ and GA₂₀ from GA₁₂ and GA₅₃, respectively (Fig. 1). These GAs are substrates for GA 3-oxidase (GA3OX) enzymes, which catalyse the 3β-hydroxylation of GA₉ to bioactive GA₄ and GA₂₀ to bioactive GA₁ (Appleford *et al.* 2006) (Fig. 1). The two classes of GA 2-oxidase (GA2OX) enzymes catalyse 2β-hydroxylation of bioactive (C₁₉) or precursor (C₂₀) GAs, respectively, at the C-2 position, resulting in their inactivation, thus reducing the pool of bioactive GAs (Schomburg *et al.*, 2003; Thomas *et al.*, 1999). GA-mediated degradation of DELLA proteins suppresses *GA20OX* and *GA3OX* expression and promotes *GA2OX* expression as a homeostatic mechanism controlling the rate of GA biosynthesis (Zentella *et al.*, 2007).

GA20OX, *GA3OX* and *GA2OX* enzymes are encoded by multigene families in the genomes of all seed plants (Kawai *et al.*, 2014). These gene families have undergone lineage-specific expansions and functional diversification. The *Arabidopsis* genome contains four *GA3OX* genes, including *AtGA3OX1* and *AtGA3OX2*, that redundantly regulate vegetative development (Mitchum *et al.*, 2006). However, paralogous *GA3OX* genes in *Arabidopsis* and *Oryzae* are grouped into different phylogenetic subclades, indicating that these families have expanded independently since the monocot-dicot divergence (Kawai *et al.*, 2014; Pearce *et al.*, 2015; Wang *et al.*, 2023).

Monocot genomes contain at least two paralogues of *GA3OX*, including highly conserved *GA3OX2* genes that play a critical role in vegetative development. In rice, a null allele of

OsGA3OX2 (d18-AD) confers a severely dwarfed growth habit, stunted stems, and wide, dark-green leaves (Itoh *et al.*, 2001; Sakamoto *et al.*, 2004).

The *GA3OX* family also underwent independent expansion and functional divergence in different monocot tribes. In rice (*Oryza sativa*), *OsGA3OX1* is expressed in anther filaments, lodicules, pollen and is required for male reproductive development (Hsieh *et al.*, 2023; Kawai *et al.*, 2022). Transcripts are also detected in the epithelium of the embryo scutellum suggesting a role in germination (Kaneko *et al.*, 2003). However, in other *Oryzae* species, such as *Oryza punctata*, the orthologous gene is expressed in roots and spikelet tissues as well as anthers, suggesting that the specialized role of *OsGA3OX1* in reproductive development has evolved recently in *Oryza sativa* (Kawai *et al.*, 2022).

Barley (*Hordeum vulgare*) and wheat genomes do not contain orthologues of *OsGA3OX1*. An independent duplication event in the Triticeae originated the orthologues *HvGA3,18OX1* in barley and *GA3OX3* in wheat (Pearce *et al.*, 2015). Both genes are highly expressed in grain tissues but encode enzymes with distinct biochemical activity. In barley, *HvGA3,18OX1* encodes a bifunctional GA 3 β ,18-dihydroxylase enzyme that catalyses the conversion of GA₉ to GA₁₃₁, while in wheat, *GA3OX3* catalyses the 3 β -hydroxylation of GA₉ to bioactive GA₄ and of GA₆₁ to GA₅₄ (Fig. 1). A tandem duplication on chromosome 2B specific to wheat-originated *GA1OX1-B1*, which encodes a GA 1-oxidase that catalyses the conversion of GA₉ to GA₆₁ (Pearce *et al.*, 2015; Wang *et al.*, 2023). In addition to GA₆₁ and GA₅₄, developing wheat grains contain their 13-hydroxy analogues GA₆₀ and GA₅₅, respectively (Gaskin *et al.*, 1980; Kirkwood and MacMillan, 1982). Based on their biochemical activity, we proposed that TaGA1OX1-B1 and TaGA3OX3 act sequentially to catalyse GA₅₄/GA₅₅ synthesis from GA₉/GA₂₀, respectively,

during grain development, although the physiological relevance of this activity remains unknown (Pearce *et al.*, 2015).

The goal of the current study was to determine the function of *GA3OX2*, *GA3OX3*, and *GAI1OX1* in wheat. Using stacked ethyl methanesulfonate (EMS)-induced loss-of-function mutant lines, we showed that *GA3OX2* activity is essential for normal vegetative and reproductive development. *ga3ox3* mutants exhibited reduced bioactive GA levels, grain weight and height, whereas *galox1* mutants accumulated high levels of bioactive GA and had larger grains and increased height. Natural genetic variation at the *GA3OX3-B1-GAI1OX1-B1* locus was associated with grain size in a collection of wheat landraces. Our research provides insight into the functional divergence of GA biosynthesis enzymes in wheat and highlights the potential to exploit variation in GA biosynthetic pathways for crop improvement.

MATERIALS AND METHODS

Plant materials and growth conditions

Wheat lines carrying mutations in target *GA3OX* and *GAI1OX* genes were identified from an *in silico* database of wheat EMS mutants in the 'Cadenza' genetic background (Krasileva *et al.*, 2017) (Table 1). Individual M₄ lines carrying mutations in different homoeologous copies of each target gene were combined by crossing, backcrossed to wildtype 'Cadenza' to reduce the number of background mutations, and then selfed to select wildtype and mutant sister lines for each target gene. All selected mutations introduce premature stop codons upstream of essential protein domains except the *galox1* mutant, which carries a point mutation in the 3' splice acceptor site of intron 2 (Supplementary Fig. S1). With such mutations, there is a risk that the presence of alternate in-frame splice sites can result in the translation of a functional allele.

However, the extremely low levels of GA₅₄ and GA₆₁ in these mutant lines suggest that the *galox1* allele encodes a non-functional protein.

Seeds were germinated on damp filter paper, transferred to 2 cm x 2 cm cells of Rothamsted Prescription Mix compost, then moved to 15 cm pots and grown under standard glasshouse conditions. Glasshouse phenotyping of *ga3ox2* genotypes was performed using BC₃F₂ plants. Twice-weekly foliar sprays of 10 µM GA₃ were required to initiate flowering and seed setting. Glasshouse phenotyping of *ga3ox3* genotypes was performed using BC₃F₃ plants and field experiments used BC₃F₄ and BC₃F₅ lines. Glasshouse phenotyping of *galox1* genotypes was performed using BC₅F₃ plants, and field experiments used BC₅F₄ and BC₅F₅ lines.

Glasshouse experiments

Plant height was determined in the glasshouse using a randomized extended block design consisting of four blocks of 18 pots with 3 plants per pot. The trial included 10 lines in total but only the results for *ga3ox3*, *galox1* and their corresponding wildtype controls are presented here. Each genotype was grown in two pots per block so that a total of 24 plants in 8 pots were phenotyped for each line. Mean heights were compared using one-way ANOVA with a nested blocking structure (block/pot/plant), incorporating nested mutant *vs.* wildtype contrasts for each gene. Heights were transformed to logarithms (base 10) prior to analysis to achieve variance homogeneity. Tiller number and spikelet number were measured for *ga3ox2* in a separate glasshouse trial grown as a single block and compared using Student's t-test ($N = 20$).

Inflorescence development in these lines was assessed using manual dissection and imaging on a Leica M205 FA Stereomicroscope with DFC310 FX camera and Leica LAS X software (Leica Microsystems, Milton Keynes, UK).

Field experiments

Field experiments were sown in spring 2021 and autumn 2023 at Rothamsted Research Experimental Farm in Southeast England as 1 m² plots with a seeding rate of 450 seeds/m² using standard farm practice for fertiliser and pesticides. No plant growth regulators were applied. The 2021 field trial plan comprised three replicate blocks arranged as arrays of 6 rows and 6 columns, with the complete trial arranged as 18 rows by 6 columns. Lines were allocated to plots in each trial according to a resolvable row-column design with blocking as described and additional Latinization across 'long columns' (i.e. single columns of 18 plots cutting across the replicate blocks) to allow for potential additional variation due to the direction of farming operations (perpendicular to spatial blocking). The 2023 field experiment had the same overall 18 x 6 layout as in the 2021 experiment but comprised six 3-row by 6-column replicate blocks, with long columns of 18 plots again cutting across blocks. Each trial included multiple lines but only the results for *ga3ox3*, *galox1* and their corresponding wildtype controls are presented here. An error during drilling of the 2023 trial meant that the blocks no longer contained a complete replicate of the 18 genotypes tested. However, the analysis was still able to account for the design structure, enabling an appropriate comparison of the genotypes.

Height measurements in the field were taken using a floating polystyrene disc of diameter 60 cm, taking six measurements per plot. Samples for internode length, inflorescence and grain measurements were taken from 10 randomly selected main tillers from each plot. Internode and spike lengths were measured manually between the lower bounds of each node. Grain sizes were measured on samples of ~200 grains using a MARVIN-Digital Seed Analyser (MARViTECH GmbH, Germany) running the software Marvin 6.0. Grain yield was measured at final harvest, as tonnes/ha corrected to 85% dry matter, calculated using the fresh weight of grain per plot and the

grain dry matter content. Dry matter was calculated from the fresh and dry weight of a sub-sample of approximately 80 g dried for 16 h at 105 °C. Traits measured in both field trials were first analysed for each trial separately using linear mixed models (LMMs) fitted using restricted maximum likelihood (REML), each with a one-way fixed model (line) and the random model reflecting the design/randomization structure of the trial ((block/row)*long column in each case). Data from both trials were then combined using a LMM meta-analysis with a two-way (trial*line) fixed model and allowing a separate random model for each trial. Nested mutant vs. wildtype contrasts were incorporated for each gene. The meta-analysis model allows for separate estimates of the residual variance for each experiment, as well as for the different (but algebraically identical) random models.

Spikelet number, grain number, yield and individual height components were measured only in 2023 and were analysed using an LMM fitted using REML, as described above. Nested mutant vs. wildtype contrasts were incorporated for each gene.

The Watkins collection was sown at Rothamsted Farm in two consecutive years. The 2022 Watkins experiment was sown in autumn 2021 and harvested in summer 2022. The 2023 Watkins experiment was sown in autumn 2022 and harvested in summer 2023. Lines were allocated to one of six groups according to short/tall x early/middle/late characteristics. The six groups were allocated to main plots (20 x 6 arrays of field plots) within each of three blocks according to a randomised complete block design. Within main plots, lines (of a given group) were allocated to plots according to a resolvable row-column design. The 2023 trial was designed as a resolvable row-column design with three replicate blocks of 36 rows by 24 columns, 18-row Latinization and overall size 36 rows x 72 columns. All plots were 1 m² sown at 300 seeds/m². A reduced rate of nitrogen fertiliser, 80 kg N/ha was used to reduce the risk of

lodging, and plant growth regulators were applied. Grain yield was calculated as described previously. Before harvest, 20 spikes were collected from a single plot for 618 lines in 2022 and for 810 lines in 2023, threshed using a laboratory thresher and the grain and chaff samples dried and weighed. From the data the weight of grain per spike was calculated, and from the plot grain yield the number of spikes per unit area. A separate grain sample, saved from the combine harvester, was used for grain size measurements using a Marvin seed counter. The samples were then dried at 105 °C for 16 h, weighed, and the data was used to calculate thousand-grain weight (TGW). From the TGW and grain yield the number of grains per unit area was calculated, and then using the spike population data, the number of grains per spike. From this and the chaff weight from threshing, the fruiting efficiency (grains per g of chaff) was calculated. All traits were measured in 2022 and only spikes per m², grain weight per spike and plot yield was measured in 2023. One-way ANOVA was used to determine the association between *GA3OX3-B1-GA1OX1-B1* haplotype and different phenotypic traits among the landraces. Fruiting efficiency values (Fec_CalcGbSamp_grng) were log₁₀ transformed to correct variance heterogeneity, all other traits are presented on the natural scale. Tukey's Honest Significant Difference post hoc test was used to determine significant differences between haplotype groups. Haplotypes were compiled, analysed and visualized using the package genHapR (Zhang *et al.*, 2023). Accession information, including genotype, ancestral group, and country of origin for the Watkins landraces, was previously described (Cheng *et al.*, 2024). Accessions with heterozygous base calls were excluded from the analysis. Contingency tables classified by haplotype and ancestral group or geographical region were analysed using Pearson's chi-squared test for association, with statistical significance calculated using a random permutation test as some expected values were small (< 5).

Genotyping

Plants were genotyped using PCR Allele Competitive Extension (PACE) assays specific for each induced mutation. Haplotypes at the *GA3OX3-B1-GA1OX1-B1* locus were tested using two different PACE assays (Supplementary Table S1). Assays were run using an ABI7500 real-time PCR machine using 1x low-ROX PACE genotyping master mix (3CR biosciences) using 250 ng of genomic DNA, 0.4 μM of the common primer and 0.2 μM of each specific primer (Supplementary Table S1). The programme included ten cycles of touchdown PCR (Annealing temperature ~ 63 $^{\circ}\text{C}$ dropping by 0.5 $^{\circ}\text{C}$ per cycle) and 26 cycles of standard PCR (annealing temperature ~ 57 $^{\circ}\text{C}$).

GA quantification

Seven-day-old seedling tissues were harvested from BC_3F_2 *ga3ox2* mutant and wildtype 'Cadenza' plants, including the elongating leaf sheath region of the first leaf from the base to the lamina joint, including internal tissue such as developing leaves and the meristem. Five biological replicates of each genotype were harvested. To quantify GA levels in grains, samples were harvested at 25 DPA from glasshouse-grown materials of BC_3F_2 lines of *ga3ox3* (wildtype, *ga3ox3-a1*, *ga3ox3-b1* and *ga3ox3* genotypes) and BC_3F_2 lines of wildtype and *galox1* genotypes. Freeze-dried samples (approximately 5 mg) were processed, and GAs were quantified in five (seedling) or three-four (grain) biological replicates as described previously (Urbanová *et al.*, 2013). At the same stage of grain development, targeted analysis by combined gas chromatography-mass spectrometry on a MAT95XP mass spectrometer coupled to a Trace GC (ThermoElectron) (MacMillan *et al.*, 1997) was used to detect the presence of GA_{54} in different wheat species.

Enzyme assays

Expression of *TaGA1ox1* in pET32b (Pearce *et al.*, 2015) in T7 chemically competent *E. coli* (NEB) was induced in log phase with 0.5 mM IPTG and further cultivation at 20 °C for 16 h. Centrifuged cells were resuspended in 100 mM Tris-HCl buffer pH 7.2 supplemented with 100 mM NaCl, 5% glycerol and 2 mM DTT before disruption using a cell lyser (Constant Systems) at 27 kPSI. The His-tagged TaGA1OX1 was purified on HisPur cobalt spin columns (Thermo Fisher Scientific), concentrated on Amicon centrifugal filters (Millipore) with a 30 kDa cutoff and flash frozen in liquid nitrogen.

Assays to determine K_m and k_{cat} values for GA₉ and GA₂₀ were performed as described previously (MacMillan *et al.*, 1997) with minor modifications. TaGA1ox1 was diluted to 100 nM final concentration and incubated with either substrate at 30 °C for 30 min in a 0.1-25 μM concentration range in 55 μL total volume. To stop the reaction, methanol and acetic acid were added to reach 33% and 3.3% of the total volume, respectively. The samples were analyzed by LC-MS as described previously (Urbanová *et al.*, 2013) using single ion monitoring to determine the amounts of products formed. Parameters of Michaelis-Menten kinetics were calculated using GraphPad Prism 8.

Binding affinities of GA₉ and GA₂₀ with TaGA1OX1 were determined by microscale thermophoresis on a Monolith NT.115 after labelling the enzyme with 2nd generation RED-tris-NTA dye (Nanotemper). A two-fold dilution series of both substrates was prepared, starting from 0.5 mM, and mixed with 50 nM labelled enzyme in 50 mM MOPS buffer at pH 7.5. The mixture also contained 4 mM DTT, 2.5% DMSO, 0.1% Tween-20 and 250 μM FeSO₄, while 2-oxoglutarate and ascorbate were omitted to prevent enzymatic conversion.

Sequence analysis

We used BLASTn searches to identify *GA3OX2*, *GA3OX3* and *GA1OX1* genes in the genome assemblies of sequenced wheat varieties and ancestors, including *Triticum urartu* accession G1812 (Ling *et al.*, 2018), *Aegilops longissima* accession AEG-6782-2, *Aegilops speltoides* ssp. *speltoides* accession AEG-9674-1 (Avni *et al.*, 2022), *Aegilops sharonensis* accession 1644 (line number BW_24933) (Yu *et al.*, 2022), *Aegilops tauschii* (accession AL8/78) (Luo *et al.*, 2017), *Triticum dicoccoides* 'Zavitan' (Avni *et al.*, 2017) and *Triticum durum* Svevo (Maccaferri *et al.*, 2019) as well as 13 varieties of *Triticum aestivum* (Walkowiak *et al.*, 2020) and *Triticum timopheevii* (Grewal *et al.*, 2024) (Supplementary Table S2). The microhomology tool in the online platform Triticeae Gene Tribe (Chen *et al.*, 2020) was used to present the physical location of *GA3OX* and *GA1OX1* genes.

Transcriptome analysis

Leaf sheath tissue from the grain to the top of the coleoptile was harvested from seven-day-old 'Cadenza' and *ga3ox2* mutant seedlings (four biological replicates each) and flash-frozen in liquid nitrogen. Total RNA was extracted using the Monarch® Total RNA Miniprep Kit with on-column DNase treatment (New England Biolabs, Ipswich, Massachusetts, USA). RNA quality was assessed using an Agilent RNA 6000 Nano Chip and Agilent 2100 Bioanalyzer (Agilent, Santa Clara, USA). RNA samples were sequenced using paired-end Illumina sequencing by Novogene Europe (Cambridge, UK). Sequencing reads were trimmed for quality and adapter sequences using Trimmomatic 0.39 (parameters SLIDINGWINDOW:4:20; MINLEN:50) (Bolger *et al.*, 2014), then aligned and quantified using Kallisto against the IWGSC RefSeq v2.1 annotated gene models (Zhu *et al.*, 2021). Transcript per million (TPM) values were calculated

for each gene and pairwise contrasts were made between 'Cadenza' and *ga3ox2* mutants using DESeq v2 (Love *et al.*, 2014).

RESULTS

***GA3OX2* is essential for wheat vegetative and reproductive development**

Three wheat plants carrying EMS-induced mutations introducing premature stop codons in *GA3OX2-A1*, *GA3OX2-B1* and *GA3OX2-D1*, respectively, were intercrossed, then backcrossed three times to wildtype 'Cadenza', to develop a *ga3ox2* mutant line (Table 1). All three mutant alleles encode truncated proteins that lack the essential Fe (2+) 2-ODD catalytic domain and are highly likely to be non-functional (Supplementary Fig. S1A).

In seedling tissues, bioactive GA₁ content was approximately three-fold lower in *ga3ox2* mutants than in wildtype 'Cadenza' ($P < 0.001$), whereas GA₄ was not detected in any sample (Fig. 2A, Supplementary Table S3). The *ga3ox2* mutant accumulated significantly higher levels of GA₂₀, the substrate for GA3OX2, and GA₂₉, the 2 β -hydroxylated inactivated product of GA₂₀ (Fig. 2A, Supplementary Table S3). Levels of GA₄₄ and GA₁₉ were significantly lower in the *ga3ox2* mutant, consistent with increased GA 20-oxidase activity (Fig. 2A, Supplementary Table S3). Transcript levels of *GA20OX1* and *GA20OX2* were significantly higher in *ga3ox2* mutants compared to wildtype 'Cadenza', while several *GA2OX* genes were down-regulated, consistent with reduced feedback regulation in response to low bioactive GA levels (Supplementary Table S4).

In the glasshouse, *ga3ox2* plants were severely dwarfed (previously shown in (Shani *et al.*, 2024)), had darker leaves, and significantly more tillers than wildtype plants (Figs. 2B and 2C, $P < 0.001$). Reproductive development was severely delayed in the *ga3ox2* mutant, most

prominently in the stages preceding terminal spikelet formation (Stage W3.5, (Waddington *et al.*, 1983); Supplementary Fig. S2). Upon emergence, *ga3ox2* spikes were compact, had significantly fewer spikelets than the wildtype ($P < 0.001$) and did not set seed (Figs. 2D and 2E). Twice-weekly sprays of bioactive GA₃ almost completely restored the height and fertility of *ga3ox2* mutants to wildtype levels, demonstrating that the observed phenotypes are caused by GA deficiency (Fig. 2B). Plants carrying loss-of-function mutations in two of three *GA3OX2* homoeologues were only between 1% and 9% shorter than the wildtype, demonstrating that *GA3OX2* genes exhibit functional redundancy and that mutations in all three homoeologues are required to confer a severely dwarfed phenotype (Supplementary Fig. S3). Taken together, these observations demonstrate that *GA3OX2* activity is essential for normal vegetative and reproductive development in wheat.

Generation of *ga3ox3* and *galox1* mutants

In the 'Cadenza' genome, *GA3OX3-A1* and *GA3OX3-B1* are predicted to encode full-length functional 2-ODD enzymes. However, *GA3OX3-D1* carries a 7 bp insertion in exon 2 that results in the introduction of a premature stop codon upstream of the conserved Fe (2+) 2-ODD domain and likely encodes a non-functional protein (Supplementary Fig. S1A). Therefore, wheat plants carrying EMS-induced mutations introducing premature stop codons in *GA3OX3-A1* and *GA3OX3-B1*, respectively, were intercrossed then backcrossed to develop a *ga3ox3* mutant (Table 1). A third EMS-mutant line carrying a point mutation in the 3' splice acceptor site in intron 2 of *GA1OX1-B1* was backcrossed to develop a *galox1* mutant (Table 1, Supplementary Fig. S1B). In the 'Cadenza' genome, *GA3OX3-B1* and *GA1OX1-B1* are just 3,618 bp apart on chromosome 2B (Supplementary Fig. S4), precluding the recombination of these alleles into the same background, so *ga3ox3* and *galox1* mutant lines were evaluated separately.

Sequential GA1OX1-B1 and GA3OX3 activity is required for GA₅₄ and GA₅₅ synthesis in wheat grains

Transcripts of *GA3OX3* and *GA1OX1* are detected almost exclusively in developing grain tissues (Pearce *et al.*, 2015) so we quantified GA levels in grains at 25 days post anthesis (DPA), the stage at which grain filling reaches its maximum rate. Grains of wildtype plants accumulated extremely high levels of GA₅₄ and GA₅₅ and low levels of GA₆₁ and GA₆₀ consistent with strong GA3OX3 and GA1OX1 activity in both the 13-OH and 13-H branches of the GA biosynthetic pathway (Fig. 3). By contrast, GA₅₄ and GA₅₅ levels were negligible in the *ga3ox3* mutant, and the GA3OX3 substrates GA₆₁ and GA₆₀ accumulated to high levels (Fig. 3). Notably, GA₅₄ and GA₅₅ levels were significantly reduced in the *ga3ox3-b1* mutant line ($P < 0.001$) but not in the *ga3ox3-a1* mutant line ($P > 0.05$) (Supplementary Table S5). These results demonstrate that GA3OX3 activity is required for the 3 β -hydroxylation of GA₆₁ to GA₅₄ and of GA₆₀ to GA₅₅ and that *GA3OX3-B1* contributes the majority of this activity.

The *galox1* mutant also exhibited a significant reduction in GA₅₄ and GA₅₅ levels compared to the wildtype, and neither GA₆₀ nor GA₆₁ was detected in this line, demonstrating that both GA3OX3 and GA1OX1 activity is required for GA₅₄ and GA₅₅ synthesis (Fig. 3). Since *GA1OX1* genes are only found in the B genome, we tested the capacity of different wheat species to synthesise GA₅₄. Using targeted analysis, we detected GA₅₄ in the grain of hexaploid common wheat (genomes AABBDD) and tetraploid durum wheat (*T. turgidum* subsp. *durum* (AABB)) but not in *Triticum urartu* (AA) or *Ae. tauschii* (DD) (Supplementary Fig. S5).

Changes in the concentrations of GA₅₅ and GA₆₀ in the *ga3ox3* and *galox1* mutants mirrored those of GA₅₄ and GA₆₁, but the 13-hydroxy GAs were present at lower levels than their 13-H analogues, indicating that the 13-H GA pathway predominates in wheat grain (Fig. 3). We

investigated the influence of the 13-hydroxyl group on GA 1-hydroxylase activity by incubating GA₉, GA₂₀, GA₄ and GA₁ with recombinant TaGA1OX1. GA₄ and GA₁ were not converted, further confirming the necessity for 1β-hydroxylation to precede 3β-hydroxylation in the formation of GA₅₄ and GA₅₅. The enzyme converted GA₉ to GA₆₁ and GA₂₀ to GA₆₀ with kinetic parameters displayed in Supplementary Table S6. The k_{cat}/K_m values for GA₉ and GA₂₀ were 8.7×10^{-3} and $5.1 \times 10^{-3} \mu\text{M}^{-1} \text{s}^{-1}$, respectively, indicating a slight preference for GA₉ as the substrate. The dissociation constants (K_d values) for GA₉ and GA₂₀ with TaGA1OX1 were determined using microscale thermophoresis as 1.2 and 4.8 μM , respectively (Supplementary Table S6).

Taken together, these results demonstrate that the sequential activity of GA1OX1-B1 and GA3OX3 is necessary and sufficient to catalyse GA₉/GA₂₀ → GA₆₁/GA₆₀ → GA₅₄/GA₅₅ reactions in wheat grain and that most of this activity is performed by enzymes encoded by adjacent *GA1OX1-B1* and *GA3OX3-B1* genes on chromosome 2B.

GA3OX3 and GA1OX1 activity modulates bioactive GA levels during grain development

Bioactive GA₁ and GA₄ levels were significantly lower in the *ga3ox3* mutant than in the wildtype ($P < 0.001$), demonstrating that GA3OX3 catalyses the 3β-hydroxylation of GA₂₀ to GA₁ and of GA₉ to GA₄ in wheat grain (Fig. 3, Supplementary Table S5). Levels of GA₅₁ were significantly higher in the *ga3ox3* mutant ($P < 0.001$), suggesting that in the absence of GA3OX3 activity, the substrate GA₉ is subject to higher rates of 2β-hydroxylation than in the wildtype (Fig. 3). By contrast, bioactive GA₁ and GA₄ levels were extremely high in the *galox1* mutant compared to wildtype segregants (Fig. 3). The *galox1* mutant also accumulated significantly higher levels of precursor (e.g. GA₉) and inactivated (e.g. GA₃₄) forms of GA in both the 13-H and 13-OH pathways (Fig. 3).

GA3OX3 and GA1OX1 activity regulates grain development and stem elongation

To determine how differences in grain GA levels affect plant phenotype, we evaluated *galox1* and *ga3ox3* mutants in field experiments in 2021 and 2023. Across both experiments, grains from the *galox1* mutant were significantly wider, longer and larger than the wildtype segregant, although the effects on thousand-grain weight (TGW) were inconsistent between different experiments, potentially due to environmental variation between years and the inherent variation in small plot field experiments (Figs. 4A to 4D, Supplementary Table S7). By contrast, grain width and TGW were significantly lower in the *ga3ox3* mutant than in the wildtype segregant (Figs 4A to 4D, Supplementary Table S7). Despite these differences in grain size, there were no significant differences between mutant and wildtype genotypes in yield (Supplementary Table S8). Nor were there any differences in spikelet number or grain number, suggesting these genes do not influence inflorescence development (Supplementary Table S8).

Unexpectedly, *ga3ox3* and *galox1* mutations conferred differences in plant height. The *ga3ox3* mutants were 3.0 cm and 4.5 cm shorter ($P = 0.013$) than their wildtype segregants, while the *galox1* mutants were 10.7 ($P < 0.001$) and 1.2 cm taller than their wildtype segregant lines in the 2021 and 2023 experiments, respectively (Fig. 4E, Supplementary Table S7). Changes in plant height were consistent when these lines were grown in glasshouse conditions (Supplementary Fig. S6).

To understand the basis of these height differences, we measured spike and individual internode lengths across the stem. In the *ga3ox3* mutant, the four lowest internodes were all significantly shorter than in the wildtype segregant ($P \leq 0.018$), whilst spike length was not affected (Fig. 4F, Supplementary Table S8). In the *galox1* mutant, the spike was significantly longer than the wildtype segregant ($P = 0.036$), and the peduncle and P-1 internode were also longer, although

these differences were not statistically significant. The lowest three internodes were all shorter in the *galox1* mutant (Fig. 4F, Supplementary Table S8).

Taken together, our results show that the depletion of bioactive GA levels in the grains of *ga3ox3* mutants confers reduced height and TGW, while the accumulation of bioactive GA in *galox1* mutants confers increased height and larger grains.

***GA3OX2* genes are highly conserved in wheat genomes but *GA3OX3* and *GA1OX1* are genetically diverse**

We next explored the genetic variation in wheat *GA3OX* genes. *GA3OX2* presents as a homoeologous triad in the genomes of all the modern and ancestral wheat species analysed with no presence-absence variation (Supplementary Table S2). In the 'Cadenza' genome, homoeologous *GA3OX2* genes encode proteins that share >96% amino acid identity with one another (Supplementary Fig. S7). *GA3OX2* genes are also remarkably homogeneous within *T. aestivum* accessions. In the Watkins collection of 1,051 wheat varieties and landraces, a single haplotype of *GA3OX2-A1* was shared by 96.3% of accessions (Supplementary Fig. S8) and across all three *GA3OX2* homoeologues, only five polymorphisms fall in protein-coding sequences (Supplementary Fig. S8).

By contrast, *GA3OX3* and *GA1OX1* were more genetically diverse between wheat accessions. Proteins encoded by the *GA3OX3-A1* and *GA3OX3-B1* homoeologues share only 83.7% identity at the amino acid level, and *GA1OX1-B1* is even less similar (Supplementary Fig. S7).

GA3OX3-D1 was either deleted or predicted to encode a non-functional protein in all screened hexaploid wheat accessions and *Ae. tauschii* (Supplementary Table S2). Both *GA3OX3-B1* and *GA1OX1-B1* genes were found in the B genomes of all common wheat varieties, durum wheat (*T. durum*) and wild emmer wheat (*T. dicoccoides*), as well as the S genomes of *Ae. speltoides*,

Ae. sharonensis and *Ae. longissima* and the G genome of *T. timopheevii* (Supplementary Table S2). This demonstrates that the duplication that originated *GA1OX1-B1* pre-dates the domestication of common wheat.

We focused on the genetic diversity at the *GA3OX3-B1-GA1OX1-B1* locus because of their dominant role in GA biosynthesis in the grain. In the Watkins collection, 58 haplotypes at this locus were shared by two or more accessions (Supplementary Table S9). The two most common haplotypes (H1, $N = 37$ and H2, $N = 36$) were polymorphic at 362 sites, including 53 variants within the *GA3OX3-B1* and *GA1OX1-B1* coding sequence (Supplementary Table S9). The *GA3OX3-B1* proteins encoded by each haplotype share just 96.0% identity at the amino acid level, and the *GA1OX1-B1* proteins are 95.8% identical.

In addition to variation in the protein-coding sequences, three non-coding regions were deleted in H2; a region approximately 562 bp downstream of *GA1OX1-B1*, a ~1,842 bp intergenic region and a region beginning 362 bp upstream of *GA3OX3-B1* (Fig. 5A).

To study the frequency of these Indels, we selected one polymorphic site for each of the three deleted regions and re-ran haplotype analysis in the Watkins landrace collection (Fig. 5A, Supplementary Table S10). There were five haplotypes shared by more than ten accessions (Fig. 5B). Haplotypes were unevenly distributed across ancestral groups (χ^2 , 28 df = 360.77, $P < 0.001$, $N = 1022$). Across all accessions, H1, characterised by the deletion of all three regions, was the most common and was carried by 78.6% of modern wheat varieties (Fig. 5C, Supplementary Table S11). Among landraces, H1 was also the most common haplotype in all ancestral groups except groups 1 and 3, where H2, characterised by the presence of all sequences in these three regions, was the most common (Fig. 5C). H3 was carried by 31.5% of the accessions in ancestral group 6 (Fig. 5C). Haplotype frequencies also varied geographically (χ^2 ,

28 df = 349.73, $P < 0.001$, $N = 1017$). In most regions, H1 was the most common haplotype, but H2 was carried by 40.2% of lines originated in Asia and H3 was carried by 44.4% of lines originating in Australia (Supplementary Fig. S9, Supplementary Table S11).

Among landraces, variation at the *GA3OX3-B1-GA1OX1-B1* locus was associated with differences in grain width, grain area, grain weight and yield (Supplementary Table S12).

Landraces carrying H1 exhibited, on average, significantly larger and heavier grains as well as improved yield than landraces carrying H2 or H3, but were not significantly different from those carrying haplotypes H4 or H5 (Figs. 5D and 5E, Supplementary Table S12). This suggests that this locus may have been subject to selection in modern wheat varieties.

DISCUSSION

Orthologous *GA3OX2* genes play conserved roles in plant development

Genetic variation in GA biosynthesis genes has been an important source of reduced height and lodging resistance alleles in cereal crops (Hedden, 2003). These include *sd1*, a loss-of-function *OsGA20OX2* allele in rice (Sasaki *et al.*, 2002) and *Rht14*, caused by the misexpression of *TaGA2OX-A9* in wheat (Tian *et al.*, 2022). By contrast, allelic variation in *GA3OX* genes is less frequently deployed in breeding programmes, potentially because mutant alleles confer a reduction in height that is too extreme for use in crop production. The severely dwarfed phenotype of the wheat *ga3ox2* mutant is similar to the *d18-AD* and *d18-y* alleles in rice (which carry a deletion and frame-shift mutation in *OsGA3OX2*, respectively) and the *d1-6016* allele in maize (*Zea mays*) (that carries a deletion of *ZmGA3OX2*) (Itoh *et al.*, 2001; Sakamoto *et al.*, 2004; Teng *et al.*, 2013). These common phenotypes indicate that orthologous *GA3OX2* genes play functionally conserved roles in stem elongation in different cereal crops.

It is possible that mutations that reduce but do not abolish *GA3OX2* activity may have agronomic potential. For example, in rice, a 9 bp in-frame deletion in the *d18h* allele, an amino acid substitution in the *d18k* allele, and CRISPR-induced lesions in the *OsGA3OX2* promoter all confer a semi-dwarf phenotype (Itoh *et al.*, 2001; Sakamoto *et al.*, 2004; Zhou *et al.*, 2023). Similarly, in pea (*Pisum sativum*), an amino acid substitution in *LE*, which encodes a GA3OX enzyme, underlies the dwarf trait studied by Mendel (Lester *et al.*, 1997; Martin *et al.*, 1997). In maize, polymorphisms in the *ZmGA3OX2* promoter are associated with mild variation in plant height (Teng *et al.*, 2013). Mutations that introduce amino acid substitutions in wheat GA3OX2 proteins or combining loss-of-function alleles in one or two homoeologues may be one strategy to develop novel semi-dwarfing alleles for wheat production.

It is important to note that while rice plants carrying the most extreme *d18* alleles still set seeds (Itoh *et al.*, 2001; Sakamoto *et al.*, 2004) the wheat *ga3ox2* mutant is infertile (Fig. 2E). This difference is likely due to the expression profile of paralogous *GA3OX* genes in each species. Whereas *OsGA3OX1* likely contributes to 3 β -hydroxylase activity in the developing panicle (Kawai *et al.*, 2022; Sakamoto *et al.*, 2004) *TaGA3OX2* is the only wheat *GA3OX* gene expressed in the inflorescence and is therefore essential for fertility (Pearce *et al.*, 2015).

This essential role in both vegetative and reproductive development likely accounts for the extremely low levels of genetic diversity in the *GA3OX2* genes in wheat and suggests they are highly constrained evolutionarily. Therefore, while the GA-deficient *ga3ox2* mutants may prove useful as a research tool to characterise GA responses, they are unlikely to be a rich source of variation for agronomically valuable alleles in wheat.

GA3OX3 exhibits 3 β -hydroxylase activity during wheat grain development

Hormone profiling indicated that both *GA3OX3-A1* and *GA3OX3-B1* encode functional GA 3 β -hydroxylases that contribute to bioactive GA₁ and GA₄ synthesis in the developing grain (Fig. 3 and Supplementary Table S5). This is contrary to results from earlier *in vitro* studies, which detected no GA 3 β -hydroxylase activity using the recombinant GA3OX3-A1 protein, potentially due to low *in vitro* expression in the heterologous system used to test this activity (Pearce *et al.*, 2015). Although both *GA3OX2* and *GA3OX3* exhibit GA 3 β -hydroxylase activity, the phenotype of the *ga3ox3* mutant was much milder than *ga3ox2* likely because of differences in gene expression patterns. *ga3ox3* mutants exhibit a mild reduction in plant height in both field and glasshouse conditions (Fig. 4 and Supplementary Fig. S6). This finding is consistent with barley plants carrying loss-of-function mutations in the orthologue *HvGA3,18OX1*, which also exhibit reduced bioactive GA₄ levels in grain tissues and slightly reduced height (Cheng *et al.*, 2023). However, unlike the *ga3ox3* mutant in wheat, TGW was unaffected in the barley *hvgga3,18ox1* mutant (Cheng *et al.*, 2023). The difference in these observed phenotypes might arise from the functional divergence of these genes in barley and wheat. Whereas *HvGA3,18OX1* encodes a bifunctional GA 3 β ,18-dihydroxylase, catalysing the conversion of GA₉ to GA₁₃₁, GA3OX3 enzymes in wheat exhibit only 3 β -hydroxylase activity so that the mutant lines have different GA profiles (Pearce *et al.*, 2015). A tandem duplication on chromosome 2B originated *GA1OX1-B1* which encodes an enzyme with altered function in GA biosynthesis that is specific to wheat. Our genetic analyses demonstrate that GA3OX3 and GA1OX1-B1 activity is necessary and sufficient for GA_{54/55} and GA_{60/61} synthesis in wheat grains, with the 13-H pathway predominating in these tissues (Supplementary Table S5). Levels of GA₅₄ and GA₅₅ are significantly reduced in the *ga3ox3-b1* mutant but not in the *ga3ox3-a1* mutant showing that

GA3OX3-B1 is the most important enzyme catalysing these reactions (Supplementary Table S5). By contrast, GA₁ and GA₄ levels are significantly reduced in both *ga3ox3-a1* and *ga3ox3-b1* mutants, suggesting that both homoeologues contribute equally to catalyse GA₉ to GA₄ and GA₂₀ to GA₁ reactions (Supplementary Table S5). This difference could be due to protein sequence variation that allows GA3OX3-A1 to discriminate between the substrates GA₉/GA₂₀ and GA₆₀/GA₆₁, whereas GA3OX3-B1 uses either substrate indiscriminately. Therefore, the majority of the grain-specific synthesis of GA₅₄ and GA₅₅ is catalysed by the sequential activity of GA3OX3-B1 and GA1OX1-B1 proteins encoded by linked genes on chromosome 2B that are inherited in the same haplotypic block.

This duplication is ancient and pre-dates the domestication of common wheat (Supplementary Table S2). The retention of both genes in all modern wheat varieties is consistent with the functional role of this locus during wheat development. The *galox1* mutant, which lacks both GA₅₄ and GA₆₁, sheds light on the physiological relevance of this pathway. The *galox1* mutant accumulates extremely high levels of bioactive GA, exhibits slightly larger grains and an increase in the length of the spike and upper stem internodes (Fig. 4). Based on these observations, it is tempting to speculate that the dual activity of GA3OX3 and GA1OX1 enzymes in grain tissues is a mechanism to modulate bioactive GA levels during grain development, potentially to moderate its effects on excessive stem elongation, which might confer improved performance in some environments.

The absence of *GA1OX1* transcripts in peduncle tissues in 'Cadenza' suggests the possibility that bioactive GA is transported from developing grains to stem tissues during the stem elongation phase. Although there are no documented examples of GAs transported from developing seeds, GA transport is an important mechanism regulating different stages of plant growth and

development (Binenbaum *et al.*, 2018). It will be important to perform more detailed transcriptional and GA profiling to determine the basis for enhanced stem elongation in the *ga3ox3* and *galox1* mutants.

Exploiting genetic variation at the *GA3OX3-B1-GA1OX1-B1* locus

Variation in the *GA3OX3-B1-GA1OX1-B1* locus is associated with differences in grain size, grain weight and yield among common wheat landraces (Figs. 5D and 5E). Haplotype 1, which is associated with higher yields, is present at high frequencies in modern wheat germplasm, which might reflect a recent selection of this allele by breeders. However, it is also possible that these allele frequencies reflect the narrow base of selection in modern wheat germplasm. Ancestral groups 2 and 5, which contributed the most genetic diversity for modern wheat varieties (Cheng *et al.*, 2024), also exhibit a high frequency of this haplotype (Fig. 5C). Therefore, introgressing the alleles from haplotypes 4 and 5, which are rare among modern wheat accessions but are associated with high mean grain size and yield in landraces (Fig. 5, Supplementary Table S12), might be one approach to exploit novel variation at this locus.

The functional differences of the allelic variation on gene activity are less clear. The *GA3OX3-B1* and *GA1OX1-B1* proteins encoded by each allele have a low level of identity at the amino acid level and may exhibit different enzymatic activities. It is also possible that the structural rearrangements in the promoter regions of these genes confer differences in spatial or temporal expression profiles. In a panel of 30 wheat varieties (Nirmal *et al.*, 2017), both H1 and H2 alleles of *GA3OX3-B1* and *GA1OX1-B1* were expressed at high levels in grain tissues at 14 DPA (Supplementary Fig. S10).

The regulatory variation that results in the expression of these genes in vegetative tissues might account for the differences in height seen in the *galox1* and *ga3ox3* mutants, as well as the

residual levels of bioactive GA₁ detected in the *ga3ox2* mutant line (Fig. 2A). It will also be interesting to study the effects of this variation on root development where a low level of *GAI**OX1-B1* transcripts was previously detected (Ptošková *et al.*, 2022). Contrasting the expression profile of these alleles using bi-parental populations segregating for the major regulatory variants detected in this study provides an excellent system to test these hypotheses.

Accepted Manuscript

ACKNOWLEDGEMENTS

We are grateful to Andrew Mead for assistance and advice on statistical analysis and to field teams and glasshouse staff for the management of field trials and controlled environment experiments. We are further grateful for the technical assistance of Renata Plotzova during the sample preparation for UHPLC-MS/MS analysis of GA.

AUTHOR CONTRIBUTIONS

ALP, SGT, PH, SP: conceptualization; ALP, AKH, SJC, PJ, DT, AR, SP: formal analysis; PH, ALP, SGT, MJH, SP: funding acquisition; ALP, AKH, RAR, PJ, PS, DT, DS: investigation; ALP, PH, SP: project administration; MJH, AR, DS: resources; ALP, PH, SGT, SP, MJH, AR: supervision; SP, ALP, PH: visualization; SP: writing – original draft and preparation; ALP, SJC, PJ, DT, PH, SP: writing – review and editing.

CONFLICT OF INTEREST

The authors declare no conflict of interest.

FUNDING

This project was funded by the Biotechnology and Biological Sciences Research Council (BBSRC) through the Delivering Sustainable Wheat (BB/X011003/1) and Designing Future Wheat (BB/P016855/1) programmes and by the European Regional Development Fund Project No. CZ.02.01.01/00/22_008/0004581 (TowArd Next GENeration of Crops; www.tangenc.cz).

DATA AVAILABILITY

The data generated in this study and statistical analyses is provided in the manuscript and supplementary tables. All plant materials used in this study are available upon request from the corresponding author.

REFERENCES

- Appleford NEJ, Evans DJ, Lenton JR, Gaskin P, Croker SJ, Devos KM, Phillips AL, Hedden P.** 2006. Function and transcript analysis of gibberellin-biosynthetic enzymes in wheat. *Planta* **223**, 568–582.
- Avni R, Lux T, Minz-Dub A, Millet E, Sela H, Distelfeld A, Deek J, Yu G, Steuernagel B, Pozniak C, Ens J, Gundlach H, Mayer KFX, Himmelbach A, Stein N, Mascher M, Spannagl M, Wulff BBH, Sharon A.** 2022. Genome sequences of three *Aegilops* species of the section Sitopsis reveal phylogenetic relationships and provide resources for wheat improvement. *The Plant Journal* **110**, 179-192.
- Avni R, Nave M, Barad O, Baruch K, Twardziok SO, Gundlach H, Hale I, Mascher M, Spannagl M, Wiebe K, Jordan KW, Golan G, Deek J, Ben-Zvi B, Ben-Zvi G, Himmelbach A, MacLachlan RP, Sharpe AG, Fritz A, Ben-David R, Budak H, Fahima T, Korol A, Faris JD, Hernandez A, Mikel MA, Levy AA, Steffenson B, Maccaferri M, Tuberosa R, Cattivelli L, Faccioli P, Ceriotti A, Kashkush K, Pourkheirandish M, Komatsuda T, Eilam T, Sela H, Sharon A, Ohad N, Chamovitz DA, Mayer KFX, Stein N, Ronen G, Peleg Z, Pozniak CJ, Akhunov ED, Distelfeld A.** 2017. Wild emmer genome architecture and diversity elucidate wheat evolution and domestication. *Science* **357**, 93-97.
- Binenbaum J, Weinstain R, Shani E.** 2018. Gibberellin localization and transport in plants. *Trends in Plant Science* **23**, 410-421.
- Bolger AM, Lohse M, Usadel B.** 2014. Trimmomatic: a flexible trimmer for Illumina sequence data. *Bioinformatics* **30**, 2114-2120.

Castro-Camba R, Sánchez C, Vidal N, Vielba JM. 2022. Plant development and crop yield: the role of gibberellins. *Plants* **11**, 2650.

Chen Y, Song W, Xie X, Wang Z, Guan P, Peng H, Jiao Y, Ni Z, Sun Q, Guo W. 2020. A collinearity-incorporating homology inference strategy for connecting emerging assemblies in the Triticeae tribe as a pilot practice in the plant pangenomic era. *Molecular Plant* **13**, 1694-1708.

Cheng J, Hill C, Han Y, He T, Ye X, Shabala S, Guo G, Zhou M, Wang K, Li C. 2023. New semi-dwarfing alleles with increased coleoptile length by gene editing of *gibberellin 3-oxidase 1* using CRISPR-Cas9 in barley (*Hordeum vulgare* L.). *Plant Biotechnology Journal* **21**, 806-818.

Cheng S, Feng C, Wingen LU, Cheng H, Riche AB, Jiang M, Leverington-Waite M, Huang Z, Collier S, Orford S, Wang X, Awal R, Barker G, O'Hara T, Lister C, Siluveru A, Quiroz-Chávez J, Ramírez-González RH, Bryant R, Berry S, Bansal U, Bariana HS, Bennett MJ, Bicego B, Bilham L, Brown JKM, Burrridge A, Burt C, Buurman M, Castle M, Chartrain L, Chen B, Denbel W, Elkot AF, Fenwick P, Feuerhelm D, Foulkes J, Gaju O, Gauley A, Gaurav K, Hafeez AN, Han R, Horler R, Hou J, Iqbal MS, Kerton M, Kondic-Spica A, Kowalski A, Lage J, Li X, Liu H, Liu S, Lovegrove A, Ma L, Mumford C, Parmar S, Philp C, Playford D, Przewieslik-Allen AM, Sarfraz Z, Schafer D, Shewry PR, Shi Y, Slafer G, Song B, Song B, Steele D, Steuernagel B, Tailby P, Tyrrell S, Waheed A, Wamalwa MN, Wang X, Wei Y, Winfield M, Wu S, Wu Y, Wulff BBH, Xian W, Xu Y, Xu Y, Yuan Q, Zhang X, Edwards KJ, Dixon L, Nicholson P, Chayut N, Hawkesford MJ, Uauy C, Sanders D,

- Huang S, Griffiths S.** 2024. Harnessing landrace diversity empowers wheat breeding. *Nature* **632**, 823–831.
- de Lucas M, Davière JM, Rodríguez-Falcón M, Pontin M, Iglesias-Pedraz JM, Lorrain S, Fankhauser C, Blázquez MA, Titarenko E, Prat S.** 2008. A molecular framework for light and gibberellin control of cell elongation. *Nature* **451**, 480-484.
- Gaskin P, Kirkwood PS, Lenton JR, MacMillan J, Radley ME.** 1980. Identification of gibberellins in developing wheat grain. *Agricultural and Biological Chemistry* **44**, 1589-1593.
- Grewal S, Yang CY, Scholefield D, Ashling S, Ghosh S, Swarbreck D, Collins J, Yao E, Sen TZ, Wilson M, Yant L, King IP, King J.** 2024. Chromosome-scale genome assembly of bread wheat's wild relative *Triticum timopheevii*. *Scientific Data* **11**, 420.
- Hedden P.** 2003. The genes of the Green Revolution. *Trends in Genetics* **19**, 5-9.
- Hsieh KT, Wu CC, Lee SJ, Chen YH, Shiue SY, Liao YC, Liu SH, Wang IW, Tseng CS, Li WH, Wang CS, Chen LJ.** 2023. Rice *GA3ox1* modulates pollen starch granule accumulation and pollen wall development. *PLoS ONE* **18**, e0292400.
- Itoh H, Ueguchi-Tanaka M, Sentoku N, Kitano H, Matsuoka M, Kobayashi M.** 2001. Cloning and functional analysis of two gibberellin 3 β -hydroxylase genes that are differently expressed during the growth of rice. *Proceedings of the National Academy of Sciences USA* **98**, 8909-8914.
- Kaneko M, Itoh H, Inukai Y, Sakamoto T, Ueguchi-Tanaka M, Ashikari M, Matsuoka M.** 2003. Where do gibberellin biosynthesis and gibberellin signaling occur in rice plants? *The Plant Journal* **35**, 104-115.

- Kawai K, Takehara S, Kashio T, Morii M, Sugihara A, Yoshimura H, Ito A, Hattori M, Toda Y, Kojima M, Takebayashi Y, Furuumi H, Nonomura K-i, Mikami B, Akagi T, Sakakibara H, Kitano H, Matsuoka M, Ueguchi-Tanaka M.** 2022. Evolutionary alterations in gene expression and enzymatic activities of gibberellin 3-oxidase 1 in *Oryza*. *Communications Biology* **5**, 67.
- Kawai Y, Ono E, Mizutani M.** 2014. Evolution and diversity of the 2-oxoglutarate-dependent dioxygenase superfamily in plants. *The Plant Journal* **78**, 328-343.
- Kirkwood PS, MacMillan J.** 1982. Gibberellins A₆₀, A₆₁, and A₆₂ : partial syntheses and natural occurrence. *Journal of the Chemical Society, Perkin Transactions 1*, 689-697.
- Krasileva KV, Vasquez-Gross HA, Howell T, Bailey P, Paraiso F, Clissold L, Simmonds J, Ramirez-Gonzalez RH, Wang XD, Borrill P, Fosker C, Ayling S, Phillips AL, Uauy C, Dubcovsky J.** 2017. Uncovering hidden variation in polyploid wheat. *Proceedings of the National Academy of Sciences USA* **114**, E913-E921.
- Lester DR, Ross JJ, Davies PJ, Reid JB.** 1997. Mendel's stem length gene (*Le*) encodes a gibberellin 3 β -hydroxylase. *The Plant Cell* **9**, 1435-1443.
- Ling HQ, Ma B, Shi X, Liu H, Dong L, Sun H, Cao Y, Gao Q, Zheng S, Li Y, Yu Y, Du H, Qi M, Li Y, Lu H, Yu H, Cui Y, Wang N, Chen C, Wu H, Zhao Y, Zhang J, Li Y, Zhou W, Zhang B, Hu W, van Eijk MJT, Tang J, Witsenboer HMA, Zhao S, Li Z, Zhang A, Wang D, Liang C.** 2018. Genome sequence of the progenitor of wheat A subgenome *Triticum urartu*. *Nature* **557**, 424-428.
- Love MI, Huber W, Anders S.** 2014. Moderated estimation of fold change and dispersion for RNA-seq data with DESeq2. *Genome Biology* **15**, 550.

Luo MC, Gu YQ, Puiu D, Wang H, Twardziok SO, Deal KR, Huo N, Zhu T, Wang L, Wang Y, McGuire PE, Liu S, Long H, Ramasamy RK, Rodriguez JC, Van SL, Yuan L, Wang Z, Xia Z, Xiao L, Anderson OD, Ouyang S, Liang Y, Zimin AV, Perteua G, Qi P, Bennetzen JL, Dai X, Dawson MW, Müller HG, Kugler K, Rivarola-Duarte L, Spannagl M, Mayer KFX, Lu FH, Bevan MW, Leroy P, Li P, You FM, Sun Q, Liu Z, Lyons E, Wicker T, Salzberg SL, Devos KM, Dvořák J. 2017. Genome sequence of the progenitor of the wheat D genome *Aegilops tauschii*. *Nature* **551**, 498-502.

Maccaferri M, Harris NS, Twardziok SO, Pasam RK, Gundlach H, Spannagl M, Ormanbekova D, Lux T, Prade VM, Milner SG, Himmelbach A, Mascher M, Bagnaresi P, Faccioli P, Cozzi P, Lauria M, Lazzari B, Stella A, Manconi A, Gnocchi M, Moscatelli M, Avni R, Deek J, Biyiklioglu S, Frascaroli E, Corneti S, Salvi S, Sonnante G, Desiderio F, Marè C, Crosatti C, Mica E, Özkan H, Kilian B, De Vita P, Marone D, Joukhadar R, Mazzucotelli E, Nigro D, Gadaleta A, Chao S, Faris JD, Melo ATO, Pumphrey M, Pecchioni N, Milanese L, Wiebe K, Ens J, MacLachlan RP, Clarke JM, Sharpe AG, Koh CS, Liang KYH, Taylor GJ, Knox R, Budak H, Mastrangelo AM, Xu SS, Stein N, Hale I, Distelfeld A, Hayden MJ, Tuberosa R, Walkowiak S, Mayer KFX, Ceriotti A, Pozniak CJ, Cattivelli L. 2019. Durum wheat genome highlights past domestication signatures and future improvement targets. *Nature Genetics* **51**, 885-895.

MacMillan J, Ward DA, Phillips AL, Sánchez-Beltrán MJ, Gaskin P, Lange T, Hedden P. 1997. Gibberellin biosynthesis from gibberellin A₁₂-aldehyde in endosperm and embryos of *Marah macrocarpus*. *Plant Physiology* **113**, 1369-1377.

- Martin DN, Proebsting WM, Hedden P.** 1997. Mendel's dwarfing gene: cDNAs from the *Le* alleles and function of the expressed proteins. Proceedings of the National Academy of Sciences USA **94**, 8907-8911.
- Mitchum MG, Yamaguchi S, Hanada A, Kuwahara A, Yoshioka Y, Kato T, Tabata S, Kamiya Y, Sun TP.** 2006. Distinct and overlapping roles of two gibberellin 3-oxidases in Arabidopsis development. The Plant Journal **45**, 804-818.
- Nirmal RC, Furtado A, Rangan P, Henry RJ.** 2017. Fasciclin-like arabinogalactan protein gene expression is associated with yield of flour in the milling of wheat. Scientific Reports **7**, 12539.
- Pearce SP, Huttly AK, Prosser IM, Li Y-d, Vaughan SP, Gallova B, Patil A, Coghill JA, Dubcovsky J, Hedden P, Phillips AL.** 2015. Heterologous expression and transcript analysis of gibberellin biosynthetic genes of grasses reveals novel functionality in the *GA3ox* family. BMC Plant Biology **15**, 130.
- Ptošková K, Szecówka M, Jaworek P, Tarkowská D, Petřík I, Pavlović I, Novák O, Thomas SG, Phillips AL, Hedden P.** 2022. Changes in the concentrations and transcripts for gibberellins and other hormones in a growing leaf and roots of wheat seedlings in response to water restriction. BMC Plant Biology **22**, 284.
- Sakamoto T, Miura K, Itoh H, Tatsumi T, Ueguchi-Tanaka M, Ishiyama K, Kobayashi M, Agrawal GK, Takeda S, Abe K, Miyao A, Hirochika H, Kitano H, Ashikari M, Matsuoka M.** 2004. An overview of gibberellin metabolism enzyme genes and their related mutants in rice. Plant Physiology **134**, 1642-1653.

- Sasaki A, Ashikari M, Ueguchi-Tanaka M, Itoh H, Nishimura A, Swapan D, K I, Saito T, Kobayashi M, Khush G, Kitano H, Matsuoka M.** 2002. A mutant gibberellin-synthesis gene in rice. *Nature* **416**, 701.
- Schomburg FM, Bizzell CM, Lee DJ, Zeevaart JA, Amasino RM.** 2003. Overexpression of a novel class of gibberellin 2-oxidases decreases gibberellin levels and creates dwarf plants. *The Plant Cell* **15**, 151-163.
- Shani E, Hedden P, Sun T-p.** 2024. Highlights in gibberellin research: A tale of the dwarf and the slender. *Plant Physiology* **195**, 111-134.
- Shimada A, Ueguchi-Tanaka M, Nakatsu T, Nakajima M, Naoe Y, Ohmiya H, Kato H, Matsuoka M.** 2008. Structural basis for gibberellin recognition by its receptor GID1. *Nature* **456**, 520-523.
- Sponsel VM.** 2016. Signal achievements in gibberellin research: the second half-century. *Annual Plant Reviews* **49**, 1-36.
- Teng F, Zhai L, Liu R, Bai W, Wang L, Huo D, Tao Y, Zheng Y, Zhang Z.** 2013. *ZmGA3ox2*, a candidate gene for a major QTL, *qPH3.1*, for plant height in maize. *The Plant Journal* **73**, 405-416.
- Thomas SG, Phillips AL, Hedden P.** 1999. Molecular cloning and functional expression of gibberellin 2- oxidases, multifunctional enzymes involved in gibberellin deactivation. *Proceedings of the National Academy of Sciences USA* **96**, 4698-4703.
- Tian X, Xia X, Xu D, Liu Y, Xie L, Hassan MA, Song J, Li F, Wang D, Zhang Y, Hao Y, Li G, Chu C, He Z, Cao S.** 2022. *Rht24b*, an ancient variation of *TaGA2ox-A9*, reduces plant height without yield penalty in wheat. *New Phytologist* **233**, 738-750.

- Ueguchi-Tanaka M, Ashikari M, Nakajima M, Itoh H, Katoh E, Kobayashi M, Chow TY, Hsing YI, Kitano H, Yamaguchi I, Matsuoka M.** 2005. *GIBBERELLIN INSENSITIVE DWARF1* encodes a soluble receptor for gibberellin. *Nature* **437**, 693-698.
- Urbanová T, Tarkovská D, Novák O, Hedden P, Strnad M.** 2013. Analysis of gibberellins as free acids by ultra performance liquid chromatography-tandem mass spectrometry. *Talanta* **112**, 85-94.
- Waddington SR, Cartwright PM, Wall PC.** 1983. A quantitative scale of spike initial and pistil development in barley and wheat. *Annals of Botany* **51**, 119-130.
- Walkowiak S, Gao L, Monat C, Haberer G, Kassa MT, Brinton J, Ramirez-Gonzalez RH, Kolodziej MC, Delorean E, Thambugala D, Klymiuk V, Byrns B, Gundlach H, Bandi V, Siri JN, Nilsen K, Aquino C, Himmelbach A, Copetti D, Ban T, Venturini L, Bevan M, Clavijo B, Koo D-H, Ens J, Wiebe K, N'Diaye A, Fritz AK, Gutwin C, Fiebig A, Fosker C, Fu BX, Accinelli GG, Gardner KA, Fradgley N, Gutierrez-Gonzalez J, Halstead-Nussloch G, Hatakeyama M, Koh CS, Deek J, Costamagna AC, Fobert P, Heavens D, Kanamori H, Kawaura K, Kobayashi F, Krasileva K, Kuo T, McKenzie N, Murata K, Nabeka Y, Paape T, Padmarasu S, Percival-Alwyn L, Kagale S, Scholz U, Sese J, Juliana P, Singh R, Shimizu-Inatsugi R, Swarbreck D, Cockram J, Budak H, Tameshige T, Tanaka T, Tsuji H, Wright J, Wu J, Steuernagel B, Small I, Cloutier S, Keeble-Gagnère G, Muehlbauer G, Tibbets J, Nasuda S, Melonek J, Hucl PJ, Sharpe AG, Clark M, Legg E, Bharti A, Langridge P, Hall A, Uauy C, Mascher M, Krattinger SG, Handa H, Shimizu KK, Distelfeld A, Chalmers K, Keller B, Mayer KFX, Poland J, Stein N, McCartney CA, Spannagl M,**

- Wicker T, Pozniak CJ.** 2020. Multiple wheat genomes reveal global variation in modern breeding. *Nature* **588**, 277-283.
- Wang T, Li J, Jiang Y, Zhang J, Ni Y, Zhang P, Yao Z, Jiao Z, Li H, Li L, Niu Y, Li Q, Yin G, Niu J.** 2023. Wheat gibberellin oxidase genes and their functions in regulating tillering. *PeerJ* **11**:e15924.
- Yu G, Matny O, Champouret N, Steuernagel B, Moscou MJ, Hernández-Pinzón I, Green P, Hayta S, Smedley M, Harwood W, Kangara N, Yue Y, Gardener C, Banfield MJ, Olivera PD, Welch C, Simmons J, Millet E, Minz-Dub A, Ronen M, Avni R, Sharon A, Patpour M, Justesen AF, Jayakodi M, Himmelbach A, Stein N, Wu S, Poland J, Ens J, Pozniak C, Karafiátová M, Molnár I, Doležel J, Ward ER, Reuber TL, Jones JDG, Mascher M, Steffenson BJ, Wulff BBH.** 2022. *Aegilops sharonensis* genome-assisted identification of stem rust resistance gene *Sr62*. *Nature Communications* **13**, 1607.
- Zentella R, Zhang ZL, Park M, Thomas SG, Endo A, Murase K, Fleet CM, Jikumaru Y, Nambara E, Kamiya Y, Sun TP.** 2007. Global analysis of DELLA direct targets in early gibberellin signaling in *Arabidopsis*. *The Plant Cell* **19**, 3037-3057.
- Zhang R, Jia G, Diao X.** 2023. geneHapR: an R package for gene haplotypic statistics and visualization. *BMC Bioinformatics* **24**, 199.
- Zhou J, Liu G, Zhao Y, Zhang R, Tang X, Li L, Jia X, Guo Y, Wu Y, Han Y, Bao Y, He Y, Han Q, Yang H, Zheng X, Qi Y, Zhang T, Zhang Y.** 2023. An efficient CRISPR-Cas12a promoter editing system for crop improvement. *Nature Plants* **9**, 588-604.
- Zhu T, Wang L, Rimbert H, Rodriguez JC, Deal KR, De Oliveira R, Choulet F, Keeble-Gagnère G, Tibbits J, Rogers J, Eversole K, Appels R, Gu YQ, Mascher M, Dvorak**

J, Luo MC. 2021. Optical maps refine the bread wheat *Triticum aestivum* cv. Chinese Spring genome assembly. *The Plant Journal* **107**, 303-314.

Accepted Manuscript

TABLES

Table 1: EMS-induced mutations in *GA3OX2*, *GA3OX3*, and *GA1OX1* used in this study. In 'Cadenza' *GA3OX3-D1* encodes a non-functional protein due to a 7 bp insertion in exon 2 that disrupts the open reading frame.

Target gene	IWGSC v2.1 gene ID	Line number	Functional effect on the protein
<i>GA3OX2-A1</i>	<i>TraesCS3A03G0268400</i>	Cadenza1176	W149*
<i>GA3OX2-B1</i>	<i>TraesCS3B03G0336700</i>	Cadenza0110	W130*
<i>GA3OX2-D1</i>	<i>TraesCS3D03G0261200</i>	Cadenza0268	W149*
<i>GA3OX3-A1</i>	<i>TraesCS2A03G1246800</i>	Cadenza0593	W71*
<i>GA3OX3-B1</i>	<i>TraesCS2B03G1429200</i>	Cadenza1640	R172*
<i>GA3OX3-D1</i>	<i>TraesCS2D03G1203500</i>	-	-
<i>GA1OX1-B1</i>	<i>TraesCS2B03G1429000</i>	Cadenza1684	3' splice acceptor intron 2.

Accepted Manuscript

FIGURE LEGENDS

Figure 1: Late stages of the GA biosynthesis pathway in higher plants showing the activity and substrates of 2-ODD enzymes. Substrates GA₅₄, GA₅₅, GA₆₀ and GA₆₁ are detected only in wheat grain tissues. The reactions forming these substrates are highlighted in blue.

Figure 2: Functional characterisation of *ga3ox2* mutant in wheat. **(A)** Quantification of GA levels in wildtype and *ga3ox2* seedling tissues. **(B)** The phenotype of representative wildtype and *ga3ox2* plants when wildtype plants reached anthesis. The plant labelled "+ GA" was sprayed twice weekly with 10 µM GA₃. **(C)** Tiller number in wildtype and *ga3ox2* mutants (*N* = 20). **(D)** Spikelet number in wildtype and *ga3ox2* mutants (*N* = 20). **(E)** Representative spikes of wildtype and *ga3ox2* mutants taken post-anthesis. 'Cadenza' and *ga3ox2* genotypes were contrasted with a two-tailed Student's t-Test. * 0.01 < *P* < 0.05, ** 0.001 < *P* < 0.01, *** *P* < 0.001.

Figure 3: Mean GA levels in the grains of wildtype (WT) and *ga3ox3* and *galox1* mutants (MT). * indicates that values are significantly different between wildtype and mutant genotypes (*P* < 0.05) determined by two-tailed Student's t-test.

Figure 4: Phenotype of *GA3OX3* and *GA1OX1* mutants in field experiments in 2021 and 2023. **(A)** Grain width (mm). **(B)** grain length (mm). **(C)** grain area (mm²). **(D)** TGW (g). **(E)** Plant height (cm). **(F)** Length of individual stem components (mm) from the 2023 experiment. Plotted values represent predicted means ± standard error. * 0.01 < *P* < 0.05, ** 0.001 < *P* < 0.01, *** *P* < 0.001. Supplementary Tables S6 and S7 include full data and statistical analysis.

Figure 5: Natural variation at the *GA3OX3-GA1OX1* locus. **(A)** *GA3OX3-B1-GA1OX1-B1* locus in wheat. The transcriptional direction of each gene is indicated in yellow boxes and the positions of the three putative deleted regions in some varieties are highlighted in blue. Red

circles indicate the positions of three selected markers to distinguish the presence and absence of each deleted region. **(B)** Haplotype frequency in the Watkins population based on three markers ($N = 1032$). **(C)** Haplotype frequency by ancestral group ($N = 1022$). Association between *GA3OX3-B1-GA1OX1-B1* haplotype and **(D)** TGW and **(E)** Grain area in 603 accessions grown in the field in 2022. Different letters indicate significant differences ($P < 0.05$) between groups based on Tukey's HSD post hoc test.

Accepted Manuscript

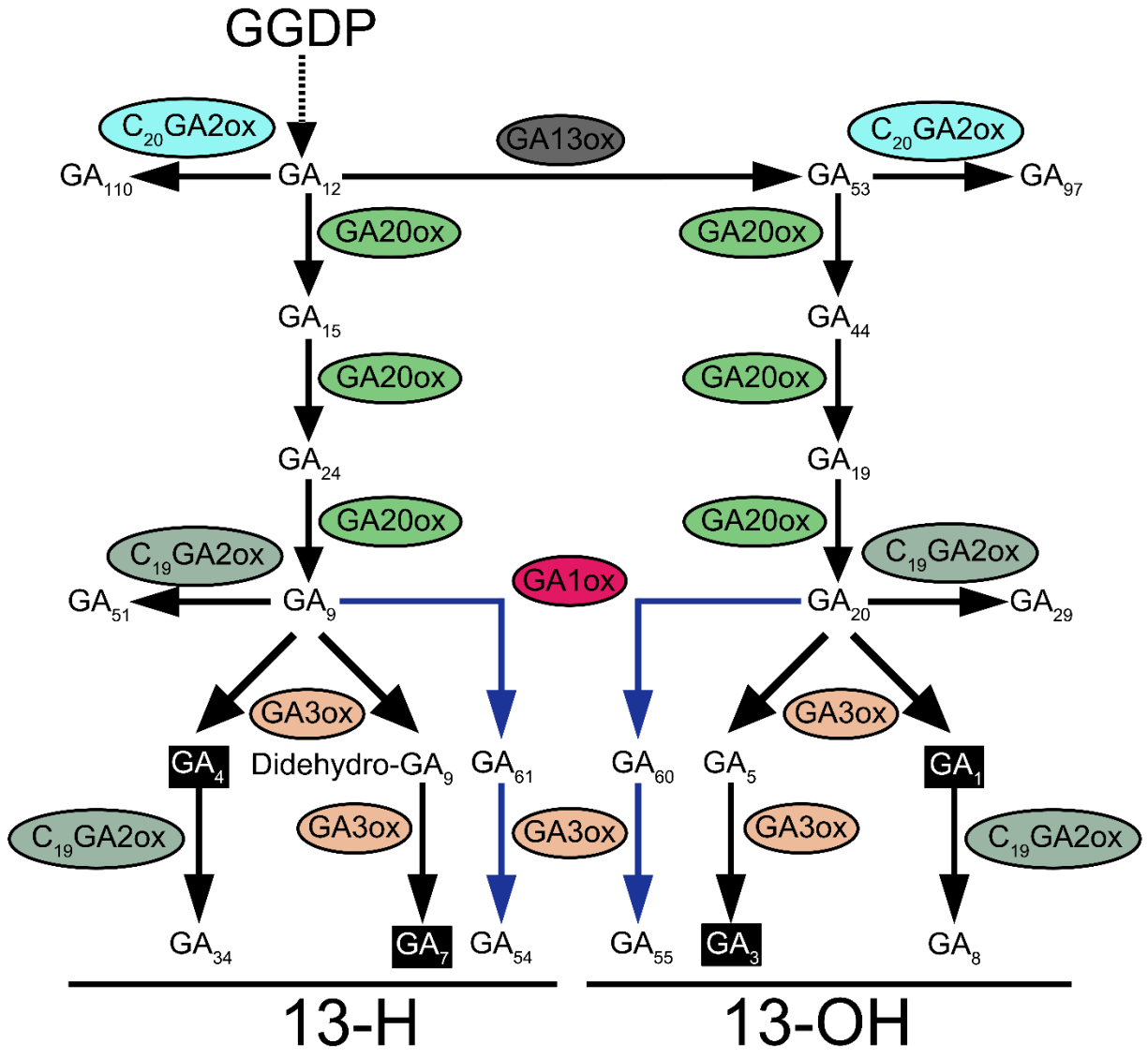


Figure 1: Late stages of the GA biosynthesis pathway in higher plants showing the activity and substrates of 2-ODD enzymes. Substrates GA₅₄, GA₅₅, GA₆₀ and GA₆₁ are detected only in wheat grain tissues. The reactions forming these substrates are highlighted in blue.

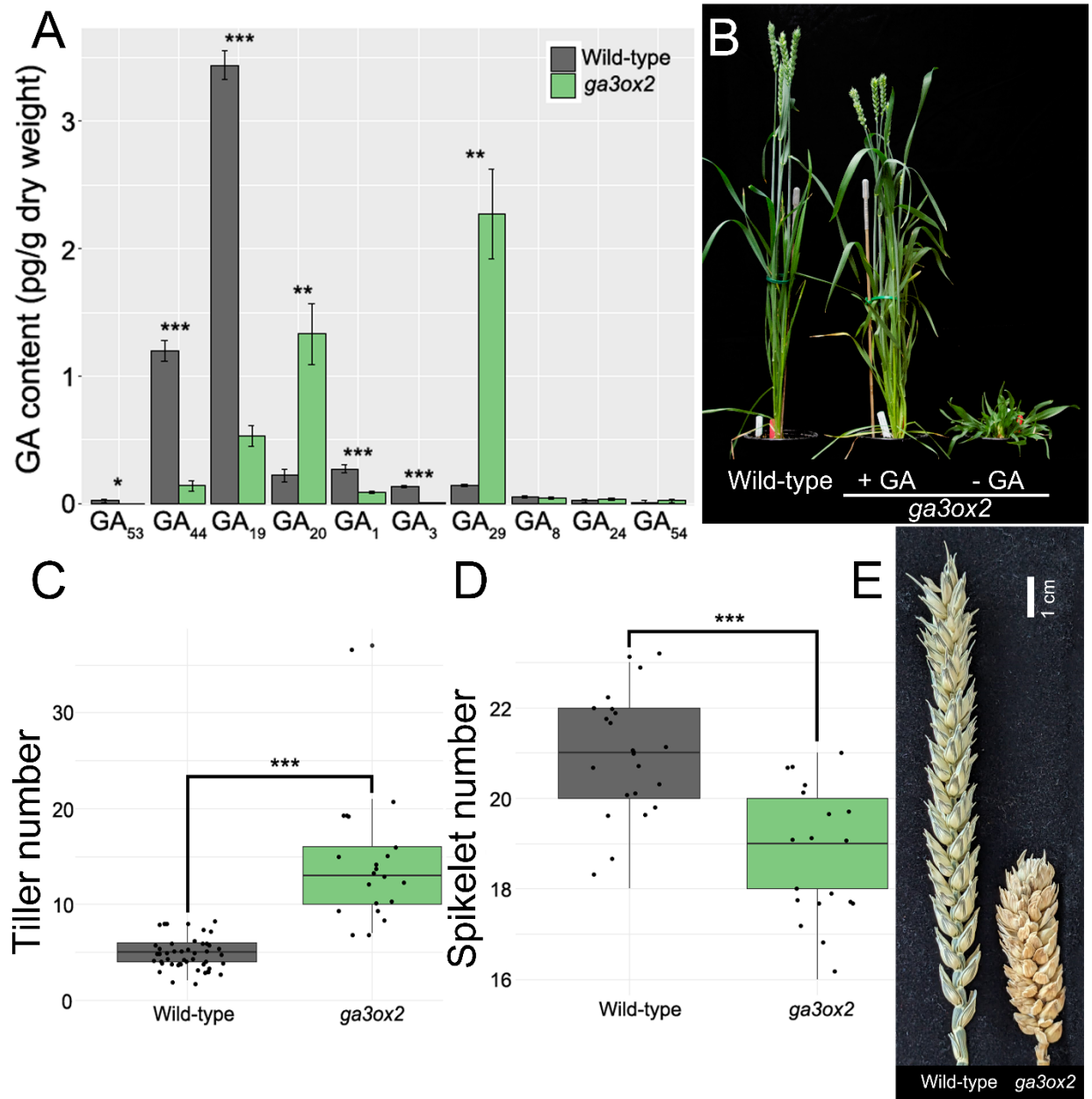


Figure 2: Functional characterisation of *ga3ox2* mutant in wheat. **(A)** Quantification of GA levels in wildtype and *ga3ox2* seedling tissues. **(B)** The phenotype of representative wildtype and *ga3ox2* plants when wildtype plants reached anthesis. The plant labelled "+ GA" was sprayed twice weekly with 10 μM GA₃. **(C)** Tiller number in wildtype and *ga3ox2* mutants (n = 20). **(D)** Spikelet number in wildtype and *ga3ox2* mutants (n =20). **(E)** Representative spikes of wildtype and *ga3ox2* mutants taken post-anthesis. 'Cadenza' and *ga3ox2* genotypes were contrasted with a two-tailed Student's T-Test * = 0.01 < P < 0.05, ** = 0.001 < P < 0.01, *** = P < 0.001.

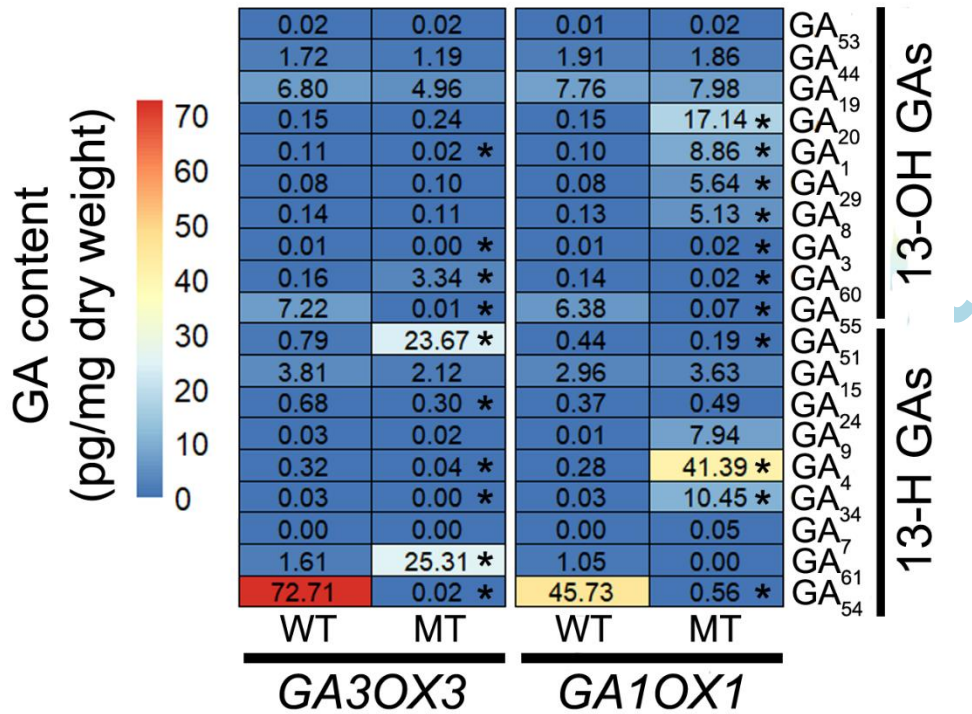


Figure 3: Mean GA levels in the grains of wildtype (WT) and *ga3ox3* and *ga1ox1* mutants (MT). * indicates that values are significantly different between wildtype and mutant genotypes ($P < 0.05$) determined by two-tailed Student's T-test.

Accepted

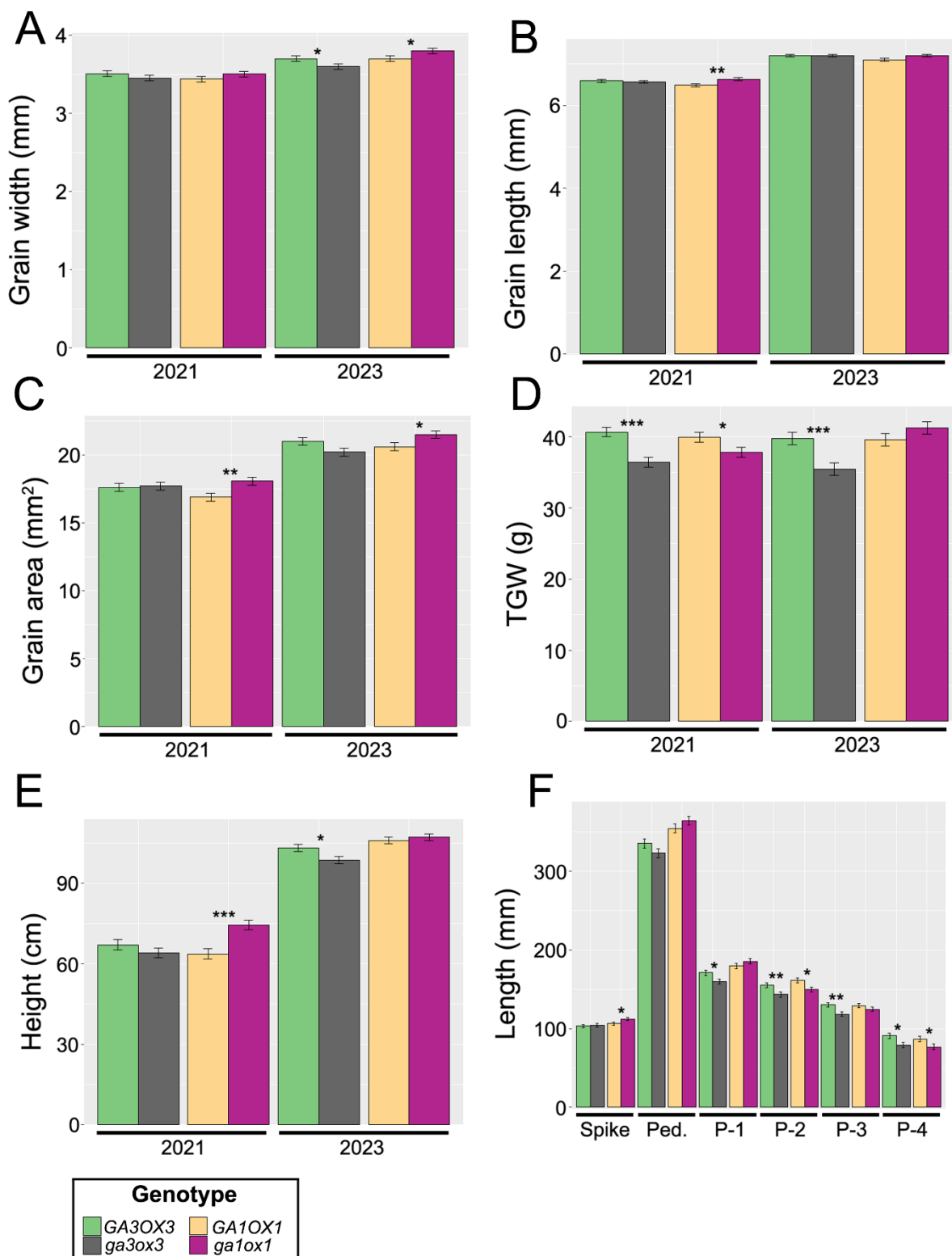


Figure 4: Phenotype of *GA3OX3* and *GA1OX1* mutants in field experiments in 2021 and 2023. **(A)** Grain width (mm). **(B)** grain length (mm). **(C)** grain area (mm²). **(D)** TGW (g). **(E)** Plot height (cm). **(F)** length of individual stem components (mm). * = 0.01 < P < 0.05, ** = 0.001 < P < 0.01, *** = P < 0.001.

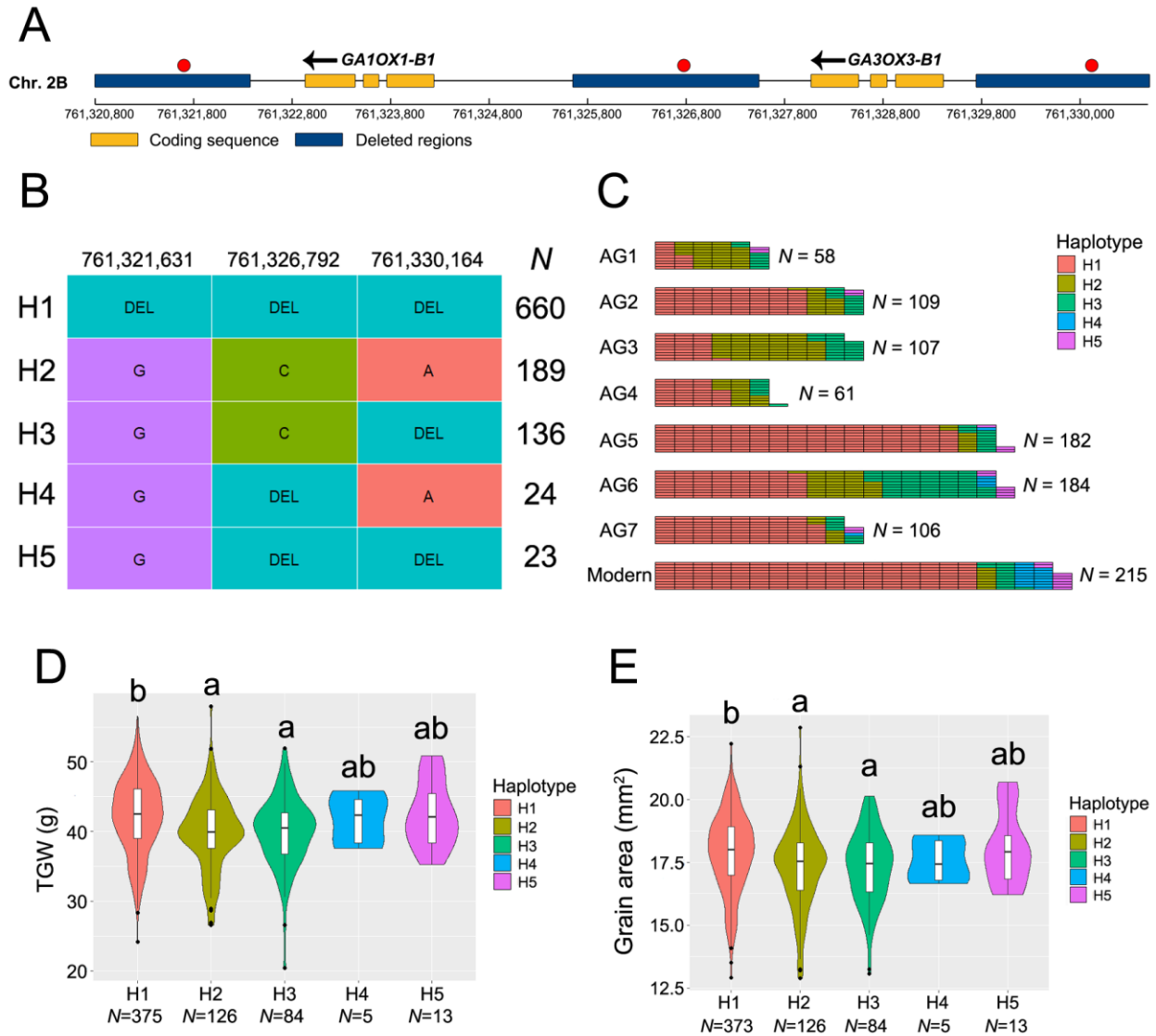


Figure 5: Natural variation at the *GA3OX3-GA1OX1* locus. **(A)** *GA3OX3-B1-GA1OX1-B1* locus in wheat. The transcriptional direction of each gene is indicated in yellow boxes and the positions of the three putative deleted regions in some varieties are highlighted in blue. Red circles indicate the positions of three selected markers to distinguish the presence and absence of each deleted region. **(B)** Haplotype frequency in the Watkins population based on three markers ($N = 1032$). **(C)** Haplotype frequency by ancestral group ($N = 1022$). Association between *GA3OX3-B1-GA1OX1-B1* haplotype and **(D)** TGW and **(E)** Grain area in 603 accessions grown in the field in 2022. Different letters indicate significant differences ($P < 0.05$) between groups based on Tukey's HSD post hoc test.